International Journal of Thermodynamics (IJoT)
ISSN 1301-9724 / e-ISSN 2146-1511
www.ijoticat.com

Vol. 23 (No. 2), pp. 128-137, 2020
doi: 10.5541/ijot.673573
Published online: June 01, 2020

Brine Management: Techno-economic Analysis of a Mechanical Vapor Compression Energy System for a Near-Zero Liquid Discharge Application

Andrea Randon[1], Sergio Rech[2,*], Andrea Lazzaretto[3]

[1,3] Department of Industrial Engineering, University of Padua, Italy
[2] Veil Energy Srl, Bolzano, Italy
E-mail: [1] andrea.randon@protonmail.com; [2] s.rech@veil-energy.eu; [3] andrea.lazzaretto@unipd.it

Received 20 Jan 2020, Revised 3 Apr 2020, Accepted 4 Apr 2020

Abstract

Fresh water availability is gradually decreasing and may limit the primary needs of drinking water and irrigation, as well as other activities, such as energy conversion, tourism, etc. A high number of desalination plants are being built to provide clean water. One of the main strategies is the brine volume minimization by means of either membrane or thermal processes. The present study focuses on the development of a techno-economic analysis of a Single Effect-Mechanical Vapor Compression (SE-MVC) system for purposes of brine volume minimization. The aim is to evaluate the thermodynamic and economic performances as well as the capital and operating expenditures of the brine concentrator when being part of a near zero liquid discharge (near-ZLD) application. This is achieved by developing the thermodynamic and economic models of the system, which are then combined together in a single integrated procedure. Brackish water analysis is used as starting point for this work. Water properties are modeled using Pitzer's equations as well as correlations found in the literature. The economic evaluation of the investment is performed by calculating the Net Present Value and Internal Rate of Return, key parameters to assess the investment viability of the project. The evaporator model provides the necessary input variables for the economic model. For a feed flow of 10.147 kg·s^{-1} and a heat duty of 18080 kW, the annualized capital cost of equipment is 594.93 k€·y^{-1}, while the operating expenses are 854.40 k€·y^{-1} The total annualized cost of the process is 1449.33 k€·y^{-1}.

Keywords: *Desalination; Single Effect Mechanical Vapor Compression (SE-MVC); Brine volume minimization; Near zero liquid discharge (near-ZLD); Techno-economic analysis.*

1. Introduction

Fresh water availability is gradually decreasing and may limit the primary needs of drinking water and irrigation, as well as other activities, such as energy conversion, tourism, etc. A high number of desalination plants are being built to provide clean water. However, brine disposal remains a matter of concern, representing an environmental and economic issue, which has to be taken in consideration from the start of the design process of a new desalination plant. In particular, the volume of the concentrate has become the main drawback of the reverse osmosis process. Among the several characteristics that render it harmful there are high salinity (and density) values, presence of ions or heavy metals and, in case of thermal processes, an elevated discharge temperature. The amount of brine in inland reverse osmosis plants is even more difficult to be disposed. Until recently, the common practice was either to discharge the brine into the sea or watercourses, directly dispose it into a water body or to inject it in an inland well. The high penalties to be paid for discharging brine in surface water have become the driving force in the search for more sustainable options.

The following main strategies have been developed to face the problem:

1. brine volume minimization, either using membrane or thermal technologies,
2. improved direct disposal;
3. reuse applications of reject brine.

The present study focuses on option 1), with specific attention to the development of a techno-economic analysis of a Single Effect Mechanical Vapor Compression (SE-MVC) evaporator. The process aims at concentrating the solution, by lowering the volume of the concentrate through evaporation of the solvent. When dealing with harsh feed water qualities, membrane processes are mainly limited by osmotic pressure and scale formation.

Attempting to overcome these problems leads to thermal processes that are more suitable to the treatment of such waters. Evaporation is not an economical process because of the high cost of technology and energy consumption, but its advantage in this field often overcomes economic issues.

An alternative solution to treat the brine could be the development of hybrid plants, which use a combination of different desalination processes, either thermal, membrane based or both combined together. The definition of the most suitable processes and the process combination in a treatment chain depends on several factors, namely the reject brine volume, the chemical composition, the geographical position of the plant, the feasibility of the process based on the capital and operating costs, the availability of storage and transportation of the brine [1]. An important contribution was given by El-Dessouky and Ettouney, who develop the models of every evaporative process involved in desalination, laying the groundwork for further developments [2]. Subsequently, H. Ettouney [3] has provided new design features of the SE-MVC system. Their

work refers to a limited concentration range of the solution, not considering the variation of the boiling point elevation (BPE) as a function of the composition of the solution, which can influence the energy consumption estimation at high concentrations. Indeed, in these types of applications where the determination of the boiling point elevation is important, it is necessary to know the osmotic coefficient, which represents the key factor to understand the solvent behaviour in such concentrated conditions. In order to obtain it, Pitzer developed a system of equations for the thermodynamic properties of electrolytes starting from and improving the Debye-Hückel model and publishing useful numerical calculations for more realistic models [4,5]. More recently, other authors have provided the basis for further developments of desalination technologies for high salinity waters. For example, Thiel et al. [6] analyze and compare the energy consumption of several desalination systems at the high salinities and diverse compositions commonly encountered in produced water from shale formations to guide the choice of the technology and address further system developments. In this context, Mechanical vapor compression (MVC) is considered one of the most established technologies, and it is widely deployed to treat high-salinity feeds [6]. They also investigate composition effects on scale formation [7]. Aqueous-NaCl solutions are also analyzed, and it is found that they closely approximate natural seawater only for salinities typically found in seawater and not for salinities found in brackish waters [8]. Mistry et al. [9] analyze the entropy generation mechanism highlighting how important it is as a tool for illustrating the influence of irreversibilities within a system on the required energy input. Lately, thermodynamic limits of the ZLD (Zero Liquid Discharge) process are evaluated and it is concluded that in terms of energy consumption, the brine concentration step has more potential for improvement than the crystallization step. The final objective of the present paper is to estimate the annualized capital (CAPEX) and operation (OPEX) costs, the Net Present Value (NPV) and the Internal Rate of Return (IRR) for the selected technology. Starting from a real water sample, the aim is reached by simulation runs of a model that (i) evaluates the boiling point elevation using the thermodynamic properties of aqueous electrolytes solutions (ii) defines the design of the system and (iii) performs the economic analysis.

2. The Mechanical Vapor Compression (MVC) System for Brine Minimization

The thermal brine minimization system is based on the distillation process, in which we can identify four main streams: the feed water to be concentrated; the generated steam, which is compressed and then used as a source of heat; distilled water and concentrate as products. Figure 1 shows the thermodynamic processes involved in the distillation process in the T-s diagram: after preheating the subcooled feed water (*2-2'*), the evaporation (*2'-3*) generates water vapor, which is then compressed (*3-4*) to allow the subsequent condensation (*4'-5*) and release the necessary heat for the evaporation in order to continue the concentration process. Figure 2 shows the thermal profiles in the evaporator.

2.1 Process Description

The process flow diagram of the Single-Effect Mechanical Vapor Compression system is shown in Figure 3. The system includes: the evaporator/condenser, a mechanical compressor, brine and distillate preheaters, circulation pumps and the venting system (the last two are not considered here for simplicity).

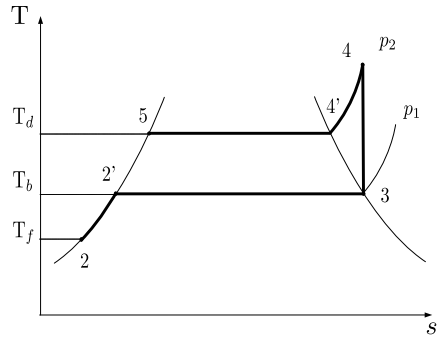

Figure 1. Thermodynamic processes involved in the distillation process (p_1 and p_2 are the evaporation and condensation pressure levels, respectively).

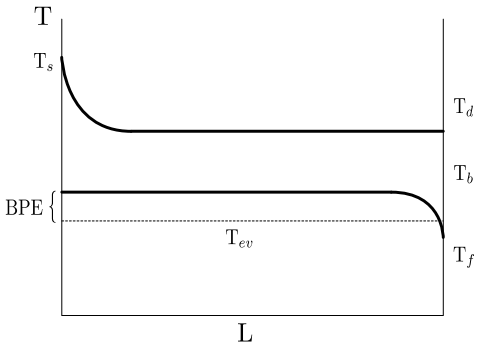

Figure 2. T-L diagram: temperature profiles through the length of the evaporator showing the effect of salinity on the boiling temperature of the water (BPE).

Condenser and evaporator form a single unit (EC in Figure 3). The two preheaters (PH) are used to recover the available heat in the effluent streams (*5-6* and *7-8*). The feed brine enters at ambient temperature and pressure ($T_{f,1}$, $p_{f,1}$ in Figure 1) and it is then split in two streams before entering the preheaters, of plate and frame type. Here, the feed brine is heated thanks to the sensible heat carried by the products (distillate and near saturation brine) leaving the evaporator. The associated temperature increase of the feed brine is important in terms of energy recovery of the system and consequently of plant efficiency. After the preheating, the feed brine enters the shell and tube EC and it is sprayed over the horizontal tube bundle through nozzles. There is a little increase in temperature of the subcooled liquid, and once the brine saturation temperature (T_b) has been reached, evaporation takes place. The change phase occurs below the atmospheric pressure, allowing evaporation to take place at lower temperature than the saturation temperature at ambient pressure. The formed steam passes through the demister and goes into a centrifugal compressor, which is used to enhance the saturation pressure of the steam and to superheat it. The superheated steam exiting the compressor flows inside the tubes of the condenser. At first it releases sensible heat reaching the saturation condition (T_d, p_d), and then it condenses yielding the latent heat to the evaporating brine that covers the outside surface of the tubes. At the end of the phase change, condensed water vapor (distillate) and near saturation brine exit the vessel and go into the preheaters to heat up the feed water.

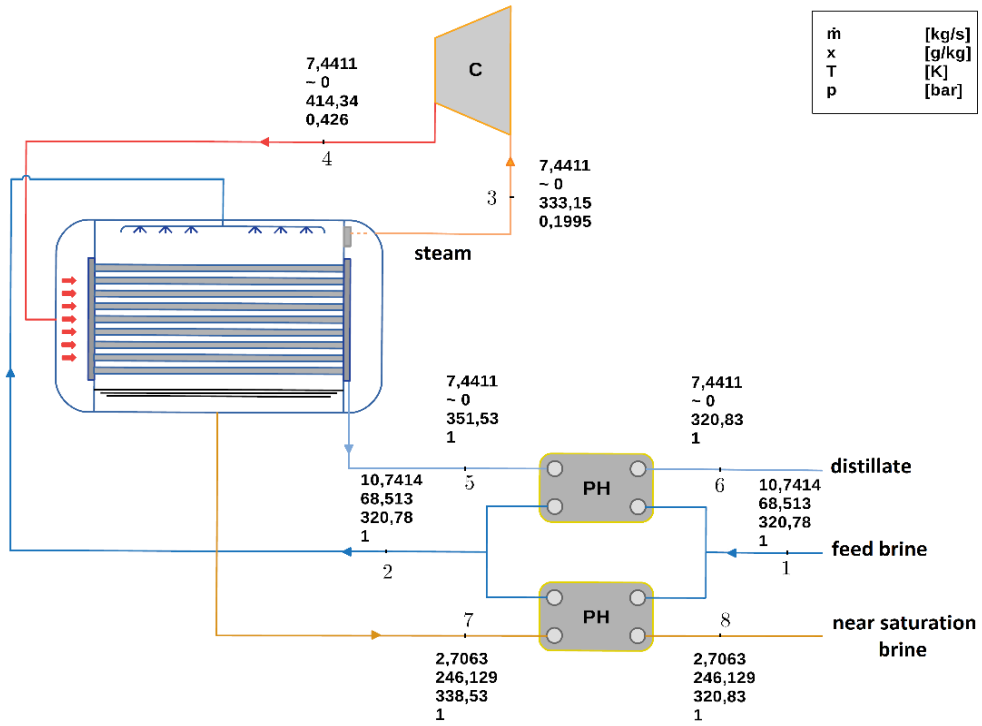

Figure 3. Schematic of the Single-Effect Mechanical Vapor Compression Desalination system. Values of the mass flow rate, concentration (on mass basis), temperature and pressure are shown in the same order as they are stated in the legend.

3. Methods

The methodology used to evaluate the capital and operating expenditure as well as performance variables of the single effect mechanical vapor compression desalination system, is based on the development of three models combined together in a single integrated procedure. The mathematical model is developed in Matlab® and a resolution algorithm is implemented to find the solution. The starting point of the analysis is a brackish water sample, supplied by Lenntech B.V.. The first model predicts the BPE. Pitzer's equations represent a reliable choice, and they are used to evaluate colligative properties of brackish water and its concentrates. A thermodynamic design model of the thermal desalination process is then developed in order to obtain performance variables along with the main inputs to the economic model. Finally, an economic model based on the module costing technique is employed to turn system performance variables into an economic value, taking into account materials of construction and operative conditions of the system.

3.1 Electrolytes Solutions Thermodynamics-Pitzer Model

The properties of a mixture that depend only on the number of solutes (i.e. concentration), and not on their nature, are called colligative. This definition is not valid when solutions are of high ionic strength and their behaviour cannot be described as ideal. In this case, it is necessary to adjust colligative properties through the osmotic coefficient (ϕ), which is used to quantify the deviation of a solvent from the ideal behaviour. When talking about thermal desalination processes, the boiling point elevation is the colligative property of interest. The exact vapor flow rate due to evaporation depends on the raising of boiling temperature. Therefore, an ion-interaction model is required to predict the osmotic coefficient of the water, which depends on the solutes' concentrations. The Pitzer's model is chosen to achieve the purpose (Appendix A). It starts from a virial expansion of the excess of the Gibbs free energy of a solution:

$$\frac{G_{ex}}{RT} = n_w[f(I) + \sum_i \sum_j \lambda_{ij}(I)\, m_i m_j + \sum_i \sum_j \sum_k \mu_{ijk}\, m_i m_j m_j] \quad (1)$$

In order to obtain the expression of the osmotic coefficient, it is necessary to take the derivative of Eq. (1) with respect to the number of moles of the solvent (the model calculates also the derivatives of Eq. (1) with respect to the number of moles of each component to evaluate their activities, but these are not of interest for the present analysis). Once the osmotic coefficient is obtained, it is easy to find the BPE using the following expression:

$$BPE = T_{sat} - T_{sat}^{o} = \frac{RT_{sat}^{o}}{r_{ev}^{o}} \phi \sum_i m_i \quad (2)$$

where R is the molar gas constant, r_{ev}^{o} and T_{sat}^{o} are the enthalpy of vaporization and the saturation temperature of pure water, respectively, while T_{sat} is the saturation temperature of the solution at fixed pressure. ϕ is the aforementioned osmotic coefficient and m_i are molalities of each solute. In most of the works concerning thermal desalination plants, interpolating relationships (given for different solution compositions) are used to find the difference between the saturation temperatures of a solution and of its pure solvent. Here it is evaluated starting from a representative water analysis of the rejected brine of a reverse osmosis process (feed brine 1 in Figure 3), which is shown in Table 1. When modelling the properties of a mixture some considerations should be made.

Considering the composition of the sample, sodium and chloride represent most of the dissolved solids, and about

95% of solutes are given by Na-Cl-Mg. All the other components are globally present as less than 5 %.

Table 1. Quality of the rejected brine of a brackish water reverse osmosis (BWRO)

Constituent		Concentration, [*mg/L*]
Name	Symbol	
Ammonium	NH_4^+	0.00
Potassium	K^+	327.99
Sodium	Na^+	16450.98
Magnesium	Ma^{2+}	4652.18
Calcium	Ca^{2+}	1813.68
Strontium	Sr^{2+}	0.00
Barium	Ba^{2+}	0.00
Carbonate	CO_3^{2-}	33.48
Bicarbonate	HCO_3^-	698.38
Nitrate	NO_3^-	3.15
Chloride	Cl^-	41561.77
Fluoride	F^-	4.30
Sulfate	SO_4^{2-}	576.45
Carbon Dioxide	CO_2	13.28
Silica	SiO_2	72.71
Boron	B	3.26
Total Dissolved Solids		66213.72

Although the other components will affect the system design through, e.g., scaling considerations, they will not affect the separation energy significantly [6]. In this work, the aforementioned ternary system is considered as NaCl-equivalent. In relation to scale formation this choice is conservative. Indeed, precipitation of sodium chloride is the main concern in the system, although additional pretreatments for brackish water sources are often required to mitigate the effects of silica and nitrates.

3.2 Thermodynamic Model of the MVC Brine Minimization System

The assumptions used to develop the thermodynamic model include the following:

1. Steady state operations;
2. The driving force for heat transfer in the evaporator is assumed to be constant and equal to the difference between condensation and evaporation temperatures;
3. The latent heats of formed vapor and condensing steam are temperature dependent;
4. The heat capacities of brine and distillate depend on temperature and composition;
5. The specific heat of the superheated vapor is constant and considered at the average temperature;
6. The preheaters have different heat transfer areas;
7. Both effluent streams exit at ambient temperature (T_0);
8. The global heat transfer coefficient in the preheaters is constant, but not equal;
9. The distillate concentration is assumed to be equal to 0 *ppm;*
10. The effect of the boiling point elevation is included in the calculations;
11. The temperature losses associated with the demister and the non-equilibrium allowance (*NEA*) are neglected;
12. The working fluid is assumed to be pure aqueous sodium chloride.

A simulation model of a single effect MVC thermal desalination plant is developed. The main input variables are shown in Table 2.

Table 2. Fixed parameters (independent variables)

Main System Specification		
x_f	68.513	*g/kg*
$p_{f,1}$	1	*bar*
$T_{f,1}$	298.15	*K*
$\dot{V}_f$	35	m^3/h
M_{NaCl}	58.4428	*g/mol*
γ	1.33	-
η_{is}	0.85	-
ΔT	10	*K*
T_{ev}	333.15	*K*
U_{ev}	3.0	$kW/(m^2\,K)$
RR_{ev}	73.33	*%*

The model can predict the variables of interest for the economic evaluation. The model follows a sequential-modular approach. Mass (Eq. (3)) and energy (Eq. (4)) balances are written for each component of the system at steady-state conditions.

$$0 = \sum_i \dot{m}_i - \sum_e \dot{m}_e \tag{3}$$

$$0 = \dot{Q} - \dot{W} + \sum_i \dot{m}_i\, h_i - \sum_e \dot{m}_e\, h_e \tag{4}$$

in which $\dot{m}_i$ and $\dot{m}_e$ are mass flow rates at inlet and outlet of the control volume, respectively. $\dot{Q}$ and $\dot{W}$ represent net rates of heat and work, while $\dot{m}_i h_i$ and $\dot{m}_e h_e$ stand for enthalpy rates through system boundary. Moreover, in the control volume comprising evaporator and compressor the concentration process is described by the salt balance (5):

$$\dot{m}_i x_i = \sum_e \dot{m}_e\, x_e \tag{5}$$

where x_i and x_e are mass concentrations of inlet and outlet streams. The model calculates temperature, pressure, mass flow rate and salinity in each point of the system. The area required by heat exchangers is calculated thanks to the heat transfer correlations (Appendix B). The power consumption of the compressor is calculated assuming the value of the isentropic efficiency. Thermophysical properties are evaluated at the average temperature of sensible heat transfer. With regard to aqueous-NaCl density and specific heat (ρ, c_p) are estimated as a function of temperature and salinity and can be found in the literature [11]. Density is calculated starting from an assumed value of the concentration (on mass basis) and iterating until convergence. The latent heats of condensation and evaporation (r_c and r_{ev}), and the enthalpy values of saturated liquid water (h_d) are calculated using correlations as a function of the temperature [2]. The specific heat of the superheated vapor is evaluated at the saturation pressure (p_d) and the average temperature between those of the superheated and condensing vapor, $(T_d + T_s)/2$. Saturation pressure and temperature are evaluated with a Matlab tool based on [12]. Thus, discharge temperatures at the exit of the preheaters (both equal to T_0) and the temperature of the feed

input to the evaporator ($T_{f,2}$) need to be initially assumed to evaluate their values iteratively using the Newton-Raphson method. The global heat transfer coefficients of the preheaters (U_d and U_b) are estimated as a function of temperature [2], while a fixed value is chosen for the global heat transfer coefficient of the evaporator (U_{ev}). The isentropic efficiency (η_{is}) of the compressor and the specific heat ratio of the vapor (γ) are considered as independent variables. It also is necessary to select the saturation temperature of pure water (T_{ev}) and the driving force of the heat transfer (ΔT), which is understood as the difference between the boiling brine temperature and the condensing vapor temperature. The recovery ratio of the evaporator (i.e., the ratio between the mass flow rates of distillate and feed brine) is chosen to be 73.33 %. When the calculation of the thermodynamic quantities of the cycle is completed, areas of heat exchangers and power consumption of the compressor are known. These variables are needed by the economic model to complete the analysis.

3.3 Economic Model

The economic model receives as input parameters the main outputs of the design model, i.e. the areas of shell and tube EC and preheaters, and the work required by the compressor. All the relevant parameters used for the economic model are reported in Table 3. The outputs of the economic model are the annualized capital and operating cost (and therefore the total annualized cost, given by the sum of the previous two terms), as well as the Net Present Value (NPV) and the Internal Rate of Return (IRR).

Table 3. Economic fixed parameters

Main Economic Parameters		
Electricity cost	0.09	*€ kWh_{el}^{-1}*
Inflation rate	3	*%*
Interest rate (i_α)	5	*%*
Average cost of a worker	50000	*€ y^{-1}*
Pure water cost	0.038 [a]	*US$ $gallon^{-1}$* [b]
Plant availability	95	*% y^{-1}*
Minimum Acceptable Rate of Return (MARR)	8 [c]	*%*
Lifetime of the project	25	*y*
Exchange rate	1.05	*€ US$$^{-1}$*

[a] taken from [13], [b] taken from [14], [c] To be intended as US gallon.

3.3.1 Capital Costs

The module costing technique is used to evaluate the fixed costs of the components of the system. This technique, which is widely described in [15], suggests that the cost of generic equipment (Bare Module Cost, C_{BM}) is related to the purchased cost of the equipment (C_P^o) assessed for certain standard conditions, such as ambient pressure and common materials. With the purpose of taking into consideration deviations from a base case, some correction factors, related to the construction materials and the operating pressure, are included in the Bare Module Factor (F_{BM}). In particular, the F_M and F_P factors have to be considered for different materials and pressures with respect to the base case. The C_P^o is calculated as a function of the component size and then actualized via the Chemical Engineering Plant Cost Index [16]. Eventually, the bare module cost of the equipment is calculated by multiplying the purchased cost of the equipment by the bare module factor, as in Eq. (6).

$$C_{BM} = C_P^o F_{BM} \tag{6}$$

The evaporator is supposed to have the shell in carbon steel and the tubes in a nickel-based alloy, which has an excellent resistance to corrosion from saltwater at high temperatures. The preheaters materials are Nickel alloy as well, and the compressor is built in carbon steel. The total cost of the equipment is calculated as the sum of the costs of the single effect of the evaporator, plus the cost of the two preheaters and the compressor. Finally, the total module cost (C_{TM}) is evaluated by adding the contingency and fee costs to the cost of equipment, which are defined as 15 % and 3 % of the cost of equipment, respectively. The auxiliary facility cost is neglected. The total module cost is annualized (CAPEX in k€ y^{-1}) using the interest rate (i_α) and assuming a certain plant amortization period (n), in accordance with Eq. (7), where the second term is defined as the *factor of annualization* (α) of the capital investment.

$$CAPEX = C_{TM}\,\alpha \tag{7}$$

$$\alpha = \frac{(1+i_\alpha)^n\, i_\alpha}{(1+i_\alpha)^n - i} \tag{8}$$

The annualized value is the amount one would have to pay at the end of each period of time (in this case the reference period is considered to be the year).

3.3.2 Operating Costs

The operating costs take into account maintenance and labor costs for maintenance, personnel costs and electricity costs. The maintenance cost is estimated as the 3% of the CAPEX (on an annual basis), while the labor cost for maintenance is defined as the 20% of the personnel cost [17]. This last term is given by the average cost of a worker multiplied by the number of required workers. The electricity cost is calculated by multiplying the specific electric consumption (calculated and equal to 1.5 kWh_{el}/m^3) by the electricity cost [18]. Finally, the thermal energy cost is not considered in this work, and it would be referred only for the startup process. The total annual operating cost (OPEX in k€ y^{-1}) is given by the sum of all the described operating cost terms.

3.3.3 Cash Flows and NPV /IRR Evaluation

The evaluation of CAPEX and OPEX performed in Sections 3.3.1 and 3.3.2 has the goal of "translating" a unique disbursement into expected annual costs. This approach is often named "annualized life cycle cost method" [19]. A deeper information about the convenience of the investment comes from the Discount Cash Flow Method. According to this method, the difference between revenues and costs (profits) in each year of the system life, are evaluated at present using an appropriate interest rate. The sum of these profits at end of the system life is called the Net Present Value (NPV), and represents a key parameter to evaluate the profitability of the investments. When talking about desalination projects, the benefits are the revenues (R_y) coming from selling the produced water (distillate) during a year, and they are defined as in Eq. (9)

$$R_1 = 365 \cdot P_w \cdot f \cdot W_p \tag{9}$$

where P_w is the amount of produced water (m^3/day), f is the plant availability specified in Table 3, and W_p is the water price (€/m^3). Regarding the costs (C_y), they comprise the

operating expenses previously described in Section 3.3.2. Then NPV is defined as

$$NPV = \sum_{y=1}^{n} \frac{R_y - C_y}{(1+i)^y} - TCC \quad (10)$$

where the investment is assumed to be concentrated in a unique outlay (and equal to the total capital investment TCC), and the cash flows (R_y-C_y) are discounted to the present day by means of an interest rate (i) equal to 3%. The internal rate of return can be a more interesting indicator as it solves Eq. (10) to calculate the required discount rate (i) for the project to break even (NPV equal to zero) considering the technical lifetime of the project (n) for which the future cash flows will be taken into account. Thus, the calculation of the IRR does not require any selection of the discount rate for the investment, actually it is the other way around, meaning that it is determined after fixing the NPV value at zero. In general, a project should be pursued when the calculated IRR is greater than the Minimum Attractive Rate of return (MARR), which is usually equal to the rate of return obtained by the company in the framework of a possible investment. In the present work a Mininimum Attractive Rate of Return equal to 8% [14] is taken into account.

4. Results

This section evaluates the mechanical vapor compressor system performances with focus on the treatment of the high salinity effluent produced in a brackish water RO process. The results are obtained by modelling the feed mixture as pure aqueous-NaCl. The feed brine flow rate is 35 m^3/h at a concentration of 68.513 g/kg.

The system operates at a recovery ratio which has to be high enough to discharge brine at near saturation conditions and it is set at 73.33%, with a fresh water production of 7.441 kg/s and a brine concentration reaching almost 246 g/kg. In addition, the required capacity of the compressor is 1010.406 kW with an isentropic efficiency equal to 0.85, and a specific work of 37.722 kWh_{el}/kg_d (or 135.787 $kW/(kg_d\ s^{-1})$). The work of the compressor is needed to enhance the pressure from 0.1995 bar (corresponding to an evaporation temperature of pure water of 333.15 K) to 0.392 bar (corresponding to a condensation temperature of pure water vapor of 348.57 K), considering that the boiling point elevation is equal to 5.38 K.

The distillate and brine preheaters require 14.658 m^2 and 4.124 m^2 heat transfer areas, respectively. The specific heat transfer area (i.e. the area of all heat exchangers needed to produce 1 kg/s of pure water) is of 83.519 $m^2/(kg_d\ s^{-1})$, while the specific heat transfer area of the evaporator is of 80.995 $m^2/(kg_d\ s^{-1})$. As regard the evaporator, the required heat duty is of 18080.61 kW.

The capital and operating expenditures at the design point are equal to 594.93 k€ y^{-1} and 854.40 k€ y^{-1}, respectively, for a comprehensive total annualized cost of 1449.33 k€ y^{-1}. The distillate is a by-product. Thus, considering a price of 0.038 US$ $gallon^{-1}$ [13], which is then converted by means of the exchange rate reported in Table 3, it can be sold at 9.34 € per cubic meter. For a mass flow rate of 7.44 kg s^{-1}, the revenue relevant to the distillate is calculated, and the cost for the electric power consumption coincide with ~40% of it.

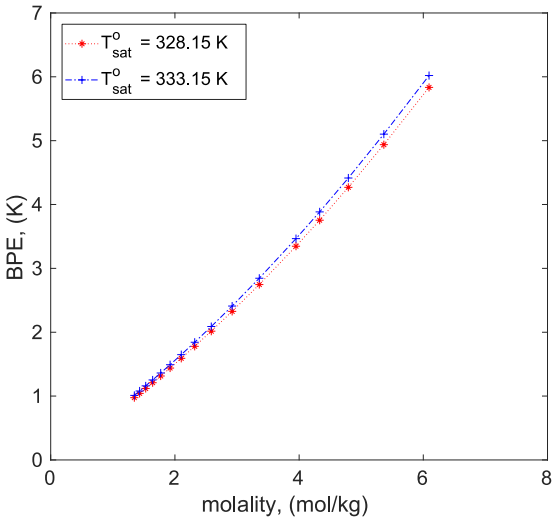

Figure 4. Influence of molality and temperature (T^o_{sat}) on the boiling point elevation (BPE).

The variation of the boiling point elevation with molality and temperature is shown in Figure 4: it is easy to see that saturation temperature does not affect too much its value; on the contrary, in this kind of applications, the contribution of molality (and therefore salinity) is not small being the concentration value high. Although for seawater processes the boiling point elevation is relatively small, for brine volume minimization purposes, it can assume larger values (due to high concentrations) which lead to a major energy consumption of the process.

The system behavior is studied by varying the main design variables. Figure 5 shows how the specific heat transfer area of the evaporator (sA_e) and the specific power consumption of the compressor (sW) vary with the temperature difference between the condensing vapor and the boiling brine (ΔT).

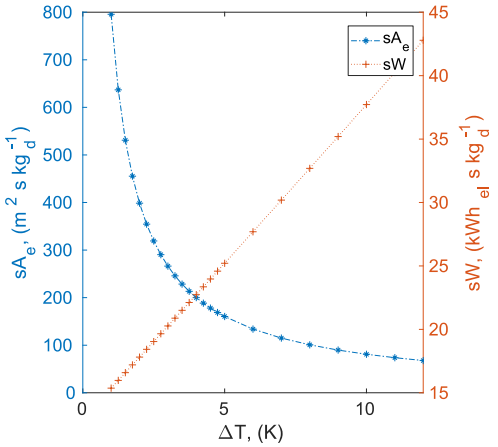

Figure 5. Influence of the temperature difference between condensing and evaporating streams (ΔT) on the specific power consumption of the comporessor (sW) and the specific heat transfer area of the evaporator (sA_e).

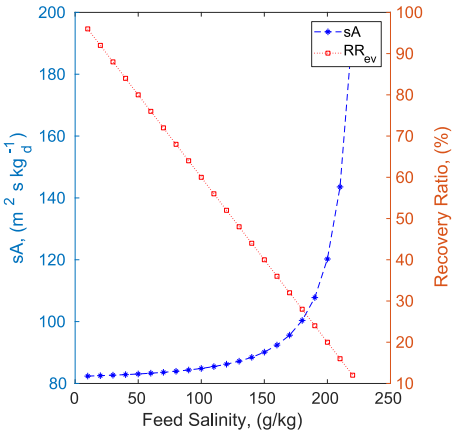

Figure 6. Comparative effect of the feed water salinity on the specific heat transfer area (to be intended as the ratio between the total area of heat exchangers and the product distillate) and recovery ratio (RR).

Note that the value of sA_e significantly affects the capital costs of the system. In fact, in this type of application where feed brine is highly corrosive, the tubes are to be made of expensive Nickel or Titanium alloy.

Figure 6 shows the effects of the increasing feed flow salinity on the recovery ratio and the specific heat transfer area of the heat exchangers for a fixed value of the near saturation brine salinity (246 g/kg). The increment of the salinity results in a reduction in the recovery ratio as the production of fresh water decreases bringing to the increase of the specific heat transfer area. As regards Figure 7, it is interesting to note that as the salinity of the feed water increases concentrating the brine, both curves of the capital and operating expenditure decrease. This fact is due to the smaller equipment size, and the consequent lower energy consumption.

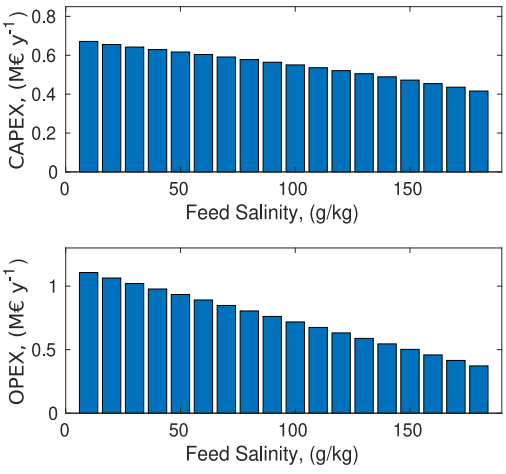

Figure 7. Effect of increasing the salinity of feed water on capital (CAPEX) and operating (OPEX) expenditure.

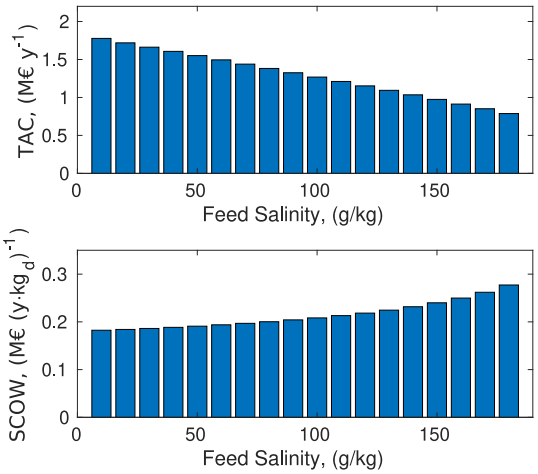

Figure 8. Effect of increasing the salinity of the feed water on total annualized cost (TAC) and simplified cost of water (SCOW).

Figure 8 shows how the simplified cost of water (defined as the ratio between the sum of CAPEX and OPEX and the product distillate) increases as the salinity of the feed water increases.

Finally, the NPV has been calculated to be positive: considering a lifetime of the project (n) of 25 years [19], and an interest rate (i) of 5%, the calculated NPV is equal to 15.029 M€. This result shows that the project is worthwhile and the system generates sufficient cash flows to repay the initial investment. Figure 10 shows the Net Present Value versus the interest rate. The intersection with the abscissa is the IRR (17.39%), which results be significantly higher than the MARR (8%). chosen by the company. The NPV corresponding to an interest rate equal to MARR is 8.97 M€.

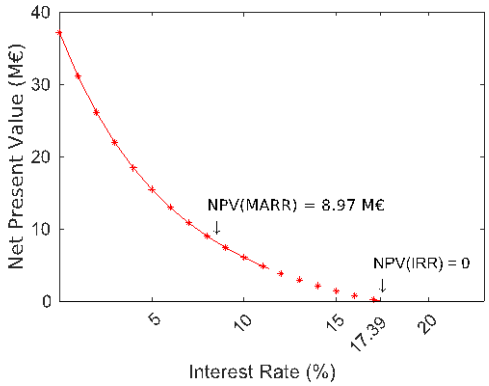

Figure 9. Net Present Value vs. Interest rate. MARR is the Minimum Attractive Rate of Return for the company (8%), IRR is the Internal Rate of Return.

5. Conclusions

A thermodynamic and economic modelling procedure has been developed to design thermal desalination systems based on mechanical vapor compression. The models are applied to a real case to evaluate the convenience this technology. Results obtained in near saturation conditions are in line with those in the market or obtained in similar works [20], indicating that the developed techno-economic procedure can be a useful tool for the economic evaluation of other similar systems.

The effect of salinity is investigated on the main economic variables, showing, in accordance with [6], how the mechanical vapor compressor system is a very suitable technology to treat harsh feed waters. The feed flow rate is 10.147 kg/s at a concentration of almost 70 g/kg. Considering a recovery ratio of 73.33 %, the fresh water flow rate is 7.441 kg/s and the total dissolved solids of the discharged brine is approximately 250 g/kg.
Finally, the economic analysis showed that:

- The capital and operating expenditures are 594.93 k€ y^{-1} and 854.40 k€ y^{-1}, respectively;
- The Net Present Value, calculated with an interest rate (i) of 5% and a lifetime (n) of 25 years, is 15.029 M€;
- The Internal Rate of Return is 17.39%.

The high Net Present Value and the significant difference between the internal and minimum attractive values of the rate of return indicate clearly the convenience of the investment.

Acknowledgements

The authors would like to thank Lenntech B.V., as well as Michele Stefani and Florent Cesarole for helpful discussions and suggestions.

Nomenclature

x	concentration, *ppm*
f	plant availability over a year, *%*
p	pressure, *bar*
h	enthalpy, *J/kg*
c_p	specific heat at constant pressure, *J/(kg K)*
U	overall heat transfer coefficient, *W/m²K*
m	molality, *mol/kg$_{solvent}$*
n	number of moles, *mol*
r	latent heat, *J/kg*
$\dot{m}$	mass flow rate, *kg/s*
T	temperature, *K*
R	molar gas constant, *J/(K mol)*
I	ionic strength
Q	heat rate, *J/s*
W	work rate (power), *J/s*
P_w	produced water, *m³/day*
W_p	water price, *€/m³*
R_y	revenues in year y, *€*
C_y	costs in year y, *€*
$f(I)$	Debye-Hückel term
G_{ex}	excess Gibbs free energy, *J/mol*
RR	recovery ratio (mass basis), *kg/kg*
EC	evaporator/condenser
NPV	net present value, *€*
IRR	internal rate of return, *%*
TAC	total annualized cost
TCC	total capital cost
TDS	total dissolved solids
BPE	boiling point elevation, *K*
BWRO	brackish water reverse osmosis
SCOW	simplified cost of water
OPEX	operating expenditure
CAPEX	annualized capital expenditure

Greek symbols

α	annualization factor
ρ	density, *kg/m³*
γ	heat capacity ratio
η	isentropic efficiency
ϕ	osmotic coefficient
λ	virial coefficient for solute pairs
μ	virial coefficient for solute triplets

Subscripts and superscripts

f	feed
d	distillate
b	brine
i	inlet
e	outlet
ev	evaporative
c	condensate
w	water
sat	saturation
0	standard state

Appendix A: Pitzer Equations and Parameters

The model is a system of equations useful to predict electrolyte thermodynamic properties, introduced by K.S. Pitzer since 1973. To this end, the Pitzer's approach begins with a virial expansion of the excess free energy (the actual free energy minus the one of an ideal solution of the same composition).

$$\frac{G_{ex}}{RT} = n_w\left[f(I) + \sum_i\sum_j \lambda_{ij}(I)\, m_i m_j + \sum_i\sum_j\sum_k \mu_{ijk}\, m_i m_j m_j\right] \quad \text{(A.1)}$$

where n_w is kilograms of water and m_i is the molality of solute i; R is the molar gas constant and T is the thermodynamic temperature. $f(I)$ represents the Debye-Hückel term and it is a function of the ionic strength $I = \frac{1}{2}\sum_i b_i z_i^2$ only, namely the electric field strength in an electrolyte solution.
The second and third virial coefficients, respectively λ_{ij} and μ_{ijk}, take in account for the short-range potential effects between solute pairs and triplets (where the second term is not relevant in this work, as it is considered only NaCl). Derivatives of (A.1) with respect of the number of moles of each of the components bring to three main equations representing the osmotic coefficient ϕ and the activity coefficients for anions and cations (γ_X and γ_M, respectively). In the following model, Eqs. (A.2) to (A.12) refer to binary aqueous electrolytes systems, and in particular for aqueous-NaCl.

$$(\phi - 1) = \frac{\frac{\partial G_{ex}}{\partial n_w}}{RT\sum_i m_i} = \\ = \frac{2}{\sum_i m_i}\left[-\frac{A^\phi I^{3/2}}{1+1.2\sqrt{I}} + \sum_c\sum_a m_c m_a\left(B_{ca}^\phi + ZC_{ca}\right)\right] \quad \text{(A.2)}$$

$$\ln\gamma_M = \frac{1}{RT}\frac{\partial G_{ex}}{\partial m_M} = \\ = z_M^2 F + \sum_a m_a(2B_{Ma} + ZC_{Ma}) + |z_M|\sum_c\sum_a m_c m_a\, C_{ca} \quad \text{(A.3)}$$

$$\ln\gamma_X = \frac{1}{RT}\frac{\partial G_{ex}}{\partial m_X} = \\ = z_X^2 F + \sum_c m_c(2B_{cX} + ZC_{cX}) + |z_X|\sum_c\sum_a m_c m_a\, C_{ca} \quad \text{(A.4)}$$

where $Z = \sum_i m_i|z_i|$. In Eqs. (A.2) to (A.4) the subscripts M and c refer to cations, X and a to anions, and i refers to all the solutes in the solution. Similarly, the summation indexes a, c and i denotes the sum over all anions, cations and solutes in the system. As mentioned before, the Pitzer model assumes functional forms of $\lambda_{ij}(I)$. They are represented by B and ϕ terms showed in Eqs. (A.2) to (A.4). Regarding Eqs. (A.3) and (A.4), the F term is defined as follows

$$F = -A^\phi\left[\frac{\sqrt{I}}{1+1.2\sqrt{I}} + \frac{2}{1.2}\ln 1 + 1.2\sqrt{I}\right] + \sum_c\sum_a m_c m_a\, B'_{ca} \quad \text{(A.4)}$$

where A^{ϕ} is related to the Debye-Hückel limiting law as follows

$$A^{\phi} = \frac{1}{3}\left[\frac{e^3(2N_0\rho_w)^{1/2}}{8\pi(\epsilon_r\epsilon_0 k_b T)^{3/2}}\right] \quad (A.6)$$

In Eq. (A.6) ρ_w and ϵ_r are the density and the relative permittivity of water, respectively, which are evaluated as shown in [20,21], e is the electron charge, N_0 is the Avogadro's number and k_b is the Boltzmann constant. T is the absolute temperature, and despite it plays a role in variations of every binary adjustable parameter ($\beta_{MX}^{(i)}$, C_{MX}^{ϕ}), A^{ϕ} is the most influenced term regarding the activity coefficients computation. Functions B_{ij}, B'_{ij}, B_{ij}^{ϕ} and C_{ij} represent interactions between anions and cations and the parameters $\beta_{MX}^{(i)}$ and C_{MX}^{ϕ} are tabulated for every given ion pair. In particular, $\beta_{MX}^{(2)}$ is relevant only for 2-2 electrolytes, in which $\alpha_1 = 1.4$ and $\alpha_1 = 12$. For 1-j type of electrolyte usually the last term of (A.7) to (A.9) are not included and $\alpha_1 = 2$. The following functional forms, dependent by ionic strength, were chosen in order to fit experimental data:

$$B_{MX}^{\phi} = \beta_{MX}^{(0)} + \beta_{MX}^{(1)} e^{-\alpha_1\sqrt{I}} + \beta_{MX}^{(2)} e^{-\alpha_2\sqrt{I}} \quad (A.7)$$

$$B_{MX} = \beta_{MX}^{(0)} + \beta_{MX}^{(1)} g(\alpha_1\sqrt{I}) + \beta_{MX}^{(2)} g(\alpha_2\sqrt{I}) \quad (A.8)$$

$$B'_{MX} = \beta_{MX}^{(1)} \frac{g'(\alpha_1\sqrt{I})}{I} + \beta_{MX}^{(2)} \frac{g'(\alpha_2\sqrt{I})}{I} \quad (A.9)$$

$$C_{MX} = \frac{C_{MX}^{\phi}}{2\sqrt{|z_M z_X|}} \quad (A.10)$$

where B'_{MX} is the derivative of B_{MX} with respect to the ionic strength, and functions g and g' are defined as

$$g(x) = \frac{2[1-(1+x)e^{-x}]}{x^2} \quad (A.11)$$

$$g'(x) = \frac{-2\left[1-\left(1+x+\frac{x^2}{2}\right)e^{-x}\right]}{x^2} \quad (A.12)$$

Appendix B: Model of the mechanical vapor compression evaporator

This appendix presents the equations of mass balances, energy balances and performance for each component of the mechanical vapor compression evaporator (see flowsheet in Figure 3).

B.1: Preheaters

Mass balance equations:

$$\dot{m}_{f,1} = \dot{m}_{f,2} = \dot{m}_f \quad (B.1)$$

$$\dot{m}_{b,3} = \dot{m}_{b,4} = \dot{m}_b \quad (B.1)$$

$$\dot{m}_{d,1} = \dot{m}_{d,2} = \dot{m}_d \quad (B.3)$$

Energy balance equation:

$$\dot{m}_f c_{p_{f,1}}(T_{f,2} - T_{f,1}) = \dot{m}_d(h_d - h_0) + \dot{m}_b c_{p_b}(T_b - T_0) \quad (B.4)$$

Performance of the distillate preheater:

$$\dot{m}_d(h_d - h_0) = A_d U_d \Delta T_{ml_d} \quad (B.5)$$

$$\Delta T_{ml_d} = \frac{(T_d - T_{f,2}) - (T_O - T_{f,1})}{\ln\left(\frac{T_d - T_{f,2}}{T_O - T_{f,1}}\right)} \quad (B.6)$$

Performance of the brine preheater:

$$\dot{m}_b c_{p_b}(T_b - T_0) = A_b U_b \Delta T_{ml_b} \quad (B.7)$$

$$\Delta T_{ml_d} = \frac{(T_b - T_{f,2}) - (T_O - T_{f,1})}{\ln\left(\frac{T_b - T_{f,2}}{T_O - T_{f,1}}\right)} \quad (B.8)$$

B.2: Evaporator

Mass and salt balance equations:

$$\dot{m}_f = \dot{m}_b + \dot{m}_d \quad (B.9)$$

$$\dot{m}_f x_f = \dot{m}_b x_b \quad (B.10)$$

Energy balance equation:

$$\dot{m}_f c_{p_f}(T_b - T_{f,2}) + \dot{m}_d r_e = \\ = \dot{m}_d r_c + m_d(h_d - h_0) + \dot{m}_b c_{p_s}(T_s - T_d) \quad (B.11)$$

Performance:

$$\dot{m}_d c_{p_s}(T_s - T_d) + \dot{m}_d r_c = A_e U_e (T_d - T_b) \quad (B.12)$$

B.3: Compressor

Mass balance equations:

$$\dot{m}_{d,7} = \dot{m}_{d,s} \quad (B.13)$$

Energy balance equation:

$$\dot{W} = (h_{d,8} - h_{d7}) \quad (B.14)$$

Performance:

$$T_s = \frac{T_{is} - T_{ev}}{\eta_{is}} + T_{ev} \quad (B.15)$$

$$T_{is} = T_s\left(\frac{p_d}{p_{ev}}\right)^{\frac{\gamma-1}{\gamma}} \quad (B.16)$$

References

[1] A. Giwa, V. Dufour, F. Al Marzooqi, M. Al Kaabi, S. W. Hasan, "Brine management methods: Recent innovations and current status" *Desalination*, *407*, 1–23, 2017.

[2] H. T. El-Dessouki, H. M. Ettouney, *Fundamentals of Salt Water Desalination*, Elsevier, 2002.

[3] H. M. Ettouney, "Design of single-effect mechanical vapor compression", *Desalination*, *190*, 1–15, 2006. https://doi.org/10.1016/j.desal.2005.08.003

[4] K. S. Pitzer, "Thermodynamics of electrolytes. I. Theoretical basis and general equation", *Journal Physical Chemistry*, *77*, 1973. https://doi.org/10.1021/j100621a026

[5] K. S. Pitzer, G. Mayorga, "Thermodynamics of electrolytes. II. Activity and osmotic coefficients for strong electrolytes with one or both ions univalent" *Journal Physical Chemistry*, *77*, 2300–2308, 1973. https://doi.org/10.1021/j100638a009

[6] G. P. Thiel, E. W. Tow, L. D. Banchik, H. W. Chung, J. H. Lienhard V., "Energy consumption in desalinating produced water from shale oil and", *Desalination*, *366*, 94–112, 2015.

http://dx.doi.org/10.1016/j.desal.2014.12.038.

[7] G. P. Thiel, J. H. Lienhard V, "Treating produced water from hydraulic fracturing: Composition effects on scale formation and desalination system selection", *Desalination*, *346*, 54–69, 2014. http://dx.doi.org/10.1016/j.desal.2014.05.001

[8] K. H. Mistry, H. A. Hunter, J. H. Lienhard V., "Effect of composition and nonideal solution behavior on desalination calculations for mixed electrolyte solutions with comparison to seawater", *Desalination*, *318*, 34-47, 2013. http://dx.doi.org/10.1016/j.desal.2013.03.015

[9] K. H. Mistry, R. K. McGovern, G. P. Thiel, E. K. Summers, S. M. Zubair, J. H. Lienhard V., "Entropy generation analysis of desalination technologies", *Entropy*, *13*, 1829-1864, 2011. https://doi.org/10.3390/e13101829

[10] H. W. Chung, K. G. Nayar, J. Swaminathan, K. M. Chehayeb, J. H. Lienhard V., "Thermodynamic analysis of brine management methods: Zero-discharge desalination and salinity-gradient power production", *Desalination*, *404*, 291–303, 2017. http://dx.doi.org/10.1016/j.desal.2016.11.022

[11] A. Ramalingam, S. Arumugam., "Experimental study on specific heat of hot brine for salt gradient solar pond application", *International Journal Chem Tech Research*, *4*, 956–961, 2012.

[12] The International Association for the Properties of Water and Steam, *Revised Release on the IAPWS Industrial Formulation 1997 for the Thermodynamic Properties of Water and Steam*. Available at: http://www.iapws.org/relguide/IF97-Rev.pdf

[13] V. C. Onishi, A. Carrero-Parreño, J. A. Reyes-Labarta, E. S. Fraga, J. A. Caballero, "Desalination of shale gas produced water: A rigorous design approach for zero-liquid discharge evaporation systems", *Journal Cleaner Production*, *140*, 1399–1414, 2017. http://dx.doi.org/10.1016/j.jclepro.2016.10.012

[14] B. Rahimi, J. May, A. Christ, K.Regenauer-Lieb, H. T. Chua, "Thermo-economic analysis of two novel low grade sensible heat driven desalination processes", *Desalination*, *365*, 316–328, 2015. http://dx.doi.org/10.1016/j.desal.2015.03.008

[15] R. Turton, R. C. Bailie, W. B. Whiting, J. A. Shaeiwitz, D. Bhattacharyya, *Analysis, Synthesis and Design of Chemical Processes*, Prentice Hall, 2008.

[16] *The annual 2018 CEPCI value*. Available at: https://ww.chemengonline.com/2019-cepci-updates-january-prelim-and-december-2018-final/

[17] T. Laukemann, F. Verdier, R. Baten, F. Trieb, M. Moser, T. Fichter, *MENA Regional Water Outlook, Phase II, Desalination using Renewable Energy*, Fichtner and DLR, 2012.

[18] *Cost of electricity for non-household consumers in the Netherlands, 2019*. Available at: https://ec.europa.eu/eurostat/statistics-explained/index.php/Electricity_price_statistics

[19] M. Papapetrou, A. Cipollina, U. La Commare, G. Micale, G. Zaragoza, G. Kosmadakis "Assessment of methodologies and data used to calculate desalination costs", *Desalination*, *419*, 8–19, 2017. http://dx.doi.org/10.1016/j.desal.2017.05.38

[20] D. J. Bradley. K. S. Pitzer, "Thermodynamics of electrolytes. 12. Dielectric properties of water and Debye-Hückel parameters to 350.degree.C and 1 kbar", *The Journal of Physical Chemistry*, *83*, 1599–1603, 1979. https://doi.org/10.1021/j100475a009

[21] G. S. Kell, "Density, thermal expansivity, and compressibility of liquid water from 0.deg. to 150.deg.. Correlations and tables for atmospheric pressure and saturation reviewed and expressed on 1968 temperature scale", *Journal of Chemical & Engineering Data*, *20*, 97–105, 1975. https://doi.org/10.1021/je60064a005